JACS
JOURNAL OF THE AMERICAN CHEMICAL SOCIETY
pubs.acs.org/JACS
Article

Mechanistic Study on Gold-Catalyzed Cycloisomerization of Dienediynes Involving Aliphatic C−H Functionalization and Inspiration for Developing a New Strategy to Access Polycarbocycles

Yi Wang, Pei-Jun Cai, and Zhi-Xiang Yu*

Cite This: J. Am. Chem. Soc. 2020, 142, 2777−2786

ABSTRACT: Previously, we developed a gold-catalyzed cycloisomerization of dienediynes to synthesize the fused 6,7,5-tricyclic compounds. This reaction involves aliphatic C−H functionalization under mild conditions with high regio- and diastereoselectivities. Herein, we present a combined density functional theory (DFT) and experimental study to understand its mechanism. The reaction starts with a 6-*endo*-dig cyclization to generate a *cis*-1-alkynyl-2-alkenylcyclopropane. Then, a Cope rearrangement takes place to give a seven-membered-ring allene intermediate, whose central carbon atom possesses vinyl cation character and thus is highly reactive toward aliphatic C−H insertion. After the C−H insertion, two successive [1,2]-hydride shifts then occur to give the tricyclic product and to complete the catalytic cycle. Notably, steric effect induced by the bulky ligand is found to be important for the diastereocontrol in the C−H insertion step. DFT calculations suggested that the malonate-tethered substrate utilized in our previous work may undergo an undesired 5-*exo*-dig cyclization under gold catalysis, which could be the reason why the desired fused 6,7,5-tricarbocyclic product was not generated. These mechanistic insights then guided us to design substrates with a shortened carbon tether in the present work to inhibit the *exo*-dig cyclization so that the tandem cyclopropanation/Cope rearrangement/C−H functionalization could occur to construct polycarbocycles containing a seven-membered ring. This prediction was supported by new experiments, providing a new strategy to access fused 5,7,5-tricyclic and 5,7,6,6-tetracyclic carbocycles. In addition, how the substituents affect the chemoselectivity was also investigated.

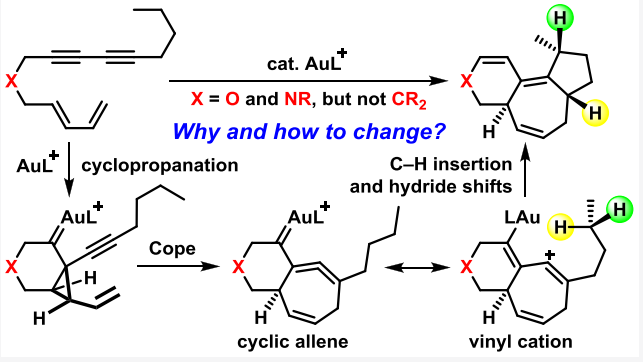

INTRODUCTION

Over the past decades, gold catalysis has become a convenient tool for the construction of molecular complexity under mild conditions.[1] Among the gold-catalyzed transformations, cycloisomerization of unsaturated hydrocarbons, such as enynes,[2] dienynes,[3] trienynes,[4] diynes,[5] allenes,[6] allenenes,[7] allenynes,[7] and allenedienes,[8] has attracted extensive attentions due to its capability of generating various types of valuable cyclic compounds from simple acyclic starting materials. Notably, these reactions have been widely applied in the synthesis of natural products and pharmaceuticals.[9]

Previously, we developed a gold-catalyzed tricyclization of dienediynes to construct fused 6,7,5-tricyclic compounds in a diastereoselective manner (Scheme 1).[10] For instance, under the catalysis of [(MeCN)Au(JohnPhos)]SbF_6 (**A**; JohnPhos = 2-(di-*tert*-butylphosphino)biphenyl), Echavarren's catalyst,[11] the cycloisomerization of oxygen-tethered dienediyne **1** proceeded smoothly at room temperature to furnish the tricyclic product **2** in 74% yield with >20:1 diastereomeric ratio (dr). In such a transformation, three stereogenic centers, three C−C bonds, and three rings are simultaneously constructed with high efficiency. It is also noteworthy that this reaction merges gold-catalyzed formal (4 + 3) cycloaddition[4,8] with C−H functionalization, which is currently one of the most prevailing research frontiers in chemistry.[12,13] The catalytic reaction of nitrogen-tethered dienediynes **3** and **5** also worked very well. One limitation of our method is that malonate-tethered substrate **7** did not give the desired product **8** under the standard conditions. In this case, other reaction products could not be identified and only the starting material was partially recovered.[14]

A catalytic cycle was previously proposed by us (Figure 1).[10] We suggested that the reaction starts with the generation of gold−substrate complex **B**, which undergoes an intramolecular cyclopropanation to form *cis*-1-alkynyl-2-alkenylcyclopropane **C**.[2] Then, a Cope rearrangement takes place, leading to cyclic allene **D**,[15] which triggers an aliphatic C−H insertion to furnish tricyclic intermediate **E**. Finally, two successive [1,2]-hydride shifts occur to complete the catalytic cycle.[16] To support or disprove this

Received: September 25, 2019
Published: January 17, 2020

Scheme 1. Gold-Catalyzed Tricyclization of Dienediynes

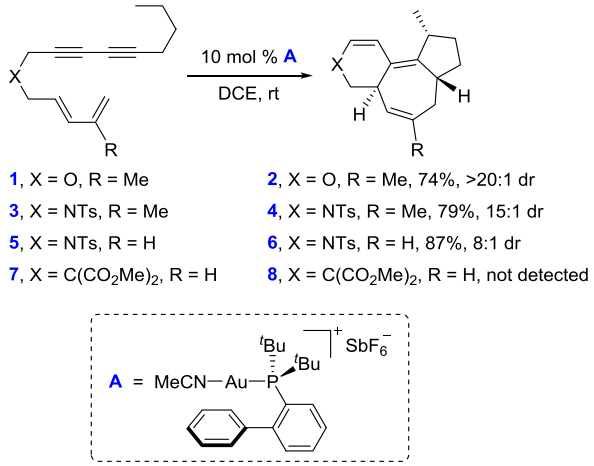

proposed mechanism, mechanistic experiments and/or theoretical calculations are required. Of equal importance, exploring how the aliphatic C−H insertion takes place and what factors control the regio- and stereoselectivities of such a step is important to understand the present reaction as well as to provide some general guidance on designing aliphatic C−H functionalization reactions.[17] Moreover, as mentioned above, carbon-tethered substrate **7** did not give the desired product **8** (Scheme 1). We envisaged that a deep mechanistic understanding of this phenomenon would help us find some solutions to overcome this hurdle and hopefully provide access to polycarbocyles containing a seven-membered ring, which are important skeletons in terpenoids.[18]

Interestingly, by using an oxygen-tethered dienediyne substrate **9** and the same gold catalyst, the Ferreira group obtained an oxabicyclo[4.1.0]heptene derivative **10** (eq 1).[19] Such a transformation was utilized as a key step in the total synthesis of gelsenicine and this reaction can be regarded as a typical enyne cycloisomerization, in which the distal alkynyl and alkenyl groups remained intact. Unlike our case, the gold-mediated Cope rearrangement (Figure 1; **C** → **D**) did not occur in Ferreira's case. In contrast, bicyclic product **10** was generated via [1,2]-hydride shift. The physical origins underlying such a mechanistic switch have not been explored yet.

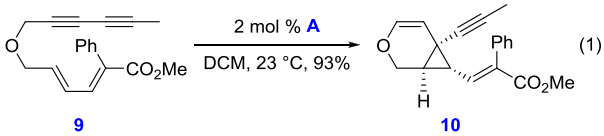

Herein, we report our mechanistic study on gold-catalyzed cycloisomerization of dienediynes based on density functional theory (DFT) calculations and deuterium labeling experiments. The detailed reaction mechanism together with the factors determining the chemo-, regio-, and stereoselectivities will be discussed. We also explored the reason why carbon-tethered substrate **7** failed to give the desired tricyclic product **8** under gold catalysis. Such an understanding then guided us to develope a new strategy to access fused 5,7,5-tricyclic and 5,7,6,6-tetracyclic carbocycles.

COMPUTATIONAL METHODS

All DFT calculations were performed with Gaussian 09 software package.[20] Pruned integration grids with 99 radial shells and 590 angular points per shell were used. Solution-phase geometry optimizations of all the stationary points were carried out using the SMD solvation model[21] and the PBE0 functional,[22] which was chosen due to its excellent

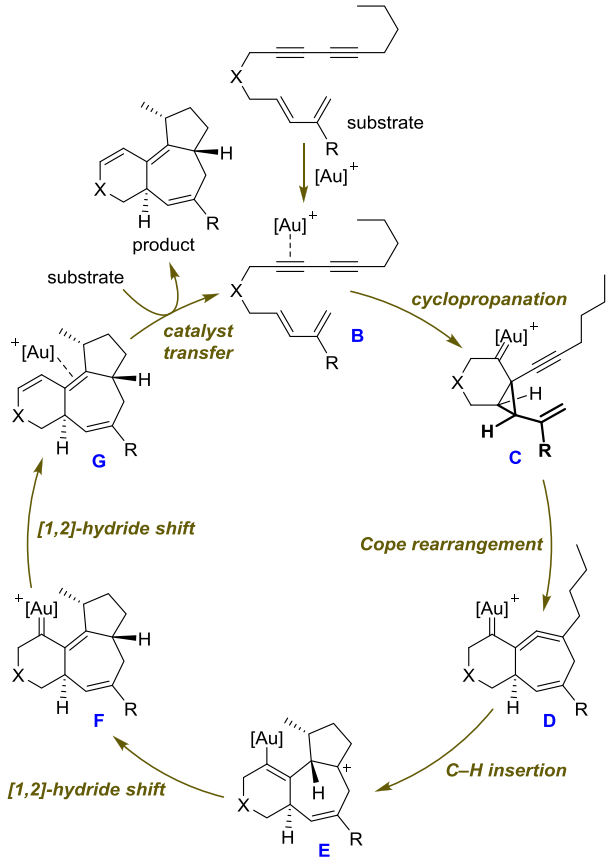

Figure 1. Proposed catalytic cycle. X = O, NTs. R = Me, H. [Au] = [Au(JohnPhos)].

performance on 5d transition metal complexes.[23] The SDD basis set (Stuttgart/Dresden ECP) was used for gold, and the 6-311G(d,p) basis set was used for the other atoms.[24] Unscaled harmonic frequency calculations at the same level were performed to validate each structure as either a minimum or a transition state and to evaluate its zero-point energy and thermal corrections at 298 K. Quasiharmonic corrections were applied during the entropy calculations by setting all positive frequencies that are less than 100 cm^{-1} to 100 cm^{-1}.[25] On the basis of the optimized structures, single-point energy refinements were performed at the SMD/BMK-D3(BJ)/def2-TZVPP level.[26−28] The BMK functional was chosen because of its high accuracy in computing the kinetics of gold-catalyzed reactions.[29] All discussed energy differences were based on Gibbs energies at 298 K (standard states are the hypothetical states at 1 mol/L) unless otherwise specified. To simplify the computations, only zigzag conformation was considered for *n*-butyl groups. Natural atomic charges were computed at the SMD(DCE)/PBE0/SDD-6-311G(d,p) level.[30] 3D structures were prepared with CYLview.[31]

RESULTS AND DISCUSSION

Mechanism of Gold-Catalyzed Tricyclization of Dienediynes. *DFT Calculations.* To simplify the computations without sacrificing the understanding of the reaction mechanism, we commenced our study by using oxygen-tethered dienediyne **1** and PMe_3 as the model substrate and ligand, respectively (see the Supporting Information for more discussion on the reaction mechanism). For nitrogen-tethered substrates (e.g., **3** and **5**) and the JohnPhos ligand, the reaction mechanism is expected to be similar (vide post). The catalytic tricyclization of dienediyne **1** starts with the catalyst transfer between $[(MeCN)Au(PMe_3)]^+$ and **1**, generating gold−alkyne complex **IN1** (in its reactive conformation[32]) and MeCN (Figure 2). Such a process is endergonic by 3.8 kcal/mol. Then, the 6-*endo*-dig cyclization of

https://dx.doi.org/10.1021/jacs.9b10362
J. Am. Chem. Soc. 2020, 142, 2777−2786

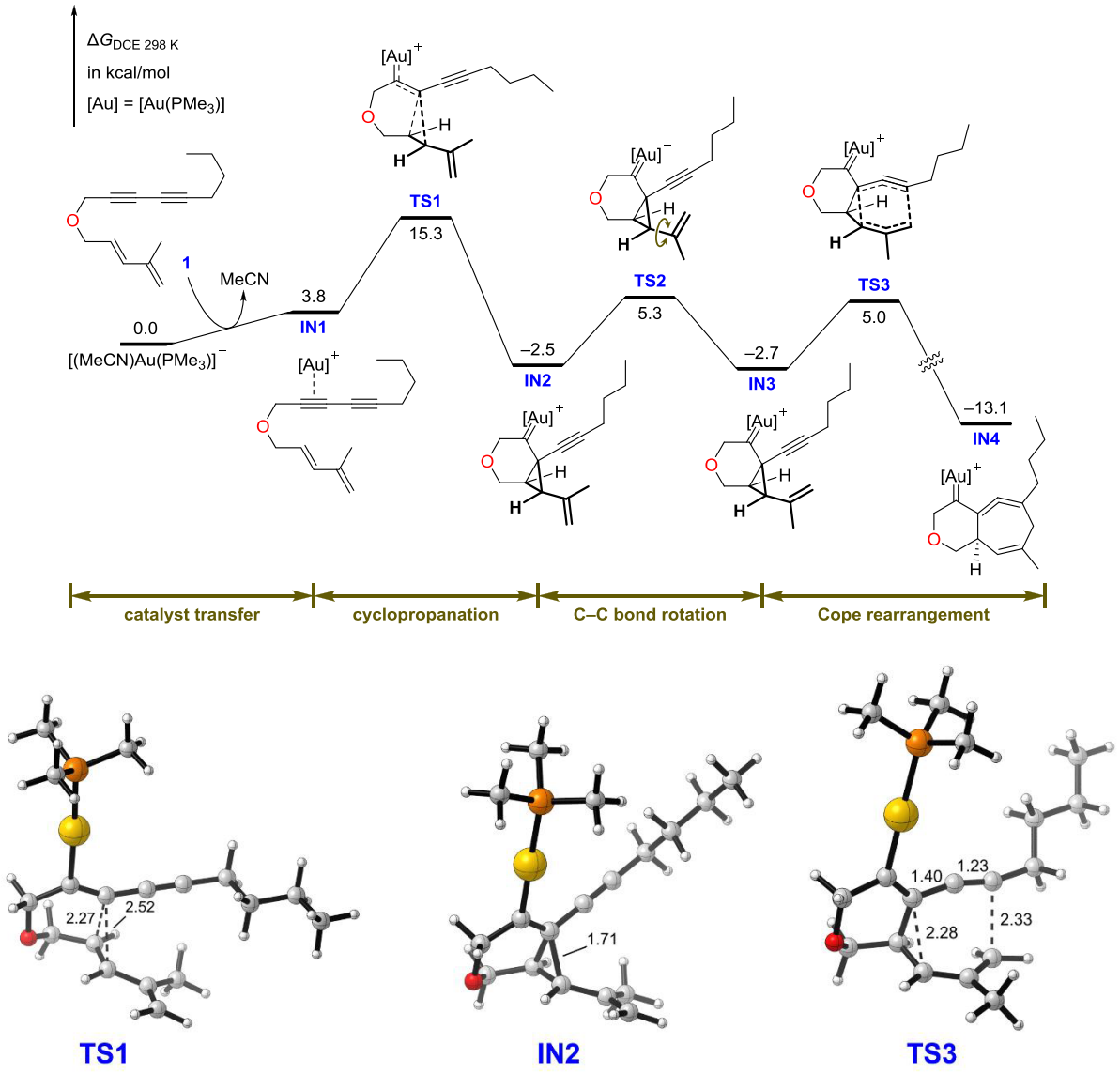

Figure 2. Gibbs energy profile for the generation of **IN4**. Computed at the SMD(DCE)/BMK-D3(BJ)/def2-TZVPP//SMD(DCE)/PBE0/SDD-6-311G(d,p) level. Color scheme: H, white; C, gray; O, red; P, orange; Au, yellow. Bond lengths are reported in Å.

IN1 occurs via cyclopropanation transition state **TS1**, leading to *cis*-1-alkynyl-2-alkenylcyclopropane **IN2**, which is not the reactive conformer for the subsequent Cope rearrangement. Therefore, **IN2** first undergoes a C−C bond rotation via **TS2** to give the reactive conformer **IN3**. Then, a fast and exergonic Cope rearrangement of **IN3** occurs via **TS3**, forming cyclic allene **IN4**.[15] Natural population analysis revealed that the central carbon atom of the allene moiety is highly electrophilic (the natural atomic charge is +0.295 e; c.f., the natural atomic charge of the central carbon atom in propadiene is +0.073 e). Furthermore, based on the presence of vacant p-type orbital on the central allenic carbon atom in the lowest unoccupied molecular orbital (LUMO) of **IN4**, we found that **IN4** is a vinyl cation in nature (Figure 3),[15b,33] making it quite different from typical seven-membered-ring allenes, which underwent dimerization to form [2 + 2] dimers rapidly even at room temperature.[15]

Then, the C−H insertion of vinyl cation **IN4** takes place via a concerted asynchronous transition state **TS4**, which closely resembles a 1,5-hydride transfer transition state (Figure 4).[34] Subsequently, the resulting C−H insertion intermediate **IN5**

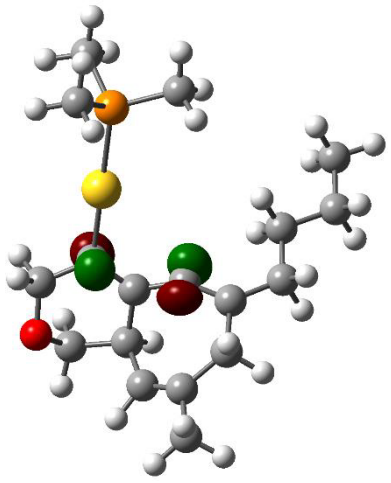

Figure 3. LUMO of **IN4** (isovalue = 0.10). Computed at the SMD(DCE)/PBE0/SDD-6-311G(d,p) level. Color scheme: H, white; C, gray; O, red; P, orange; Au, yellow.

https://dx.doi.org/10.1021/jacs.9b10362
J. Am. Chem. Soc. 2020, 142, 2777−2786

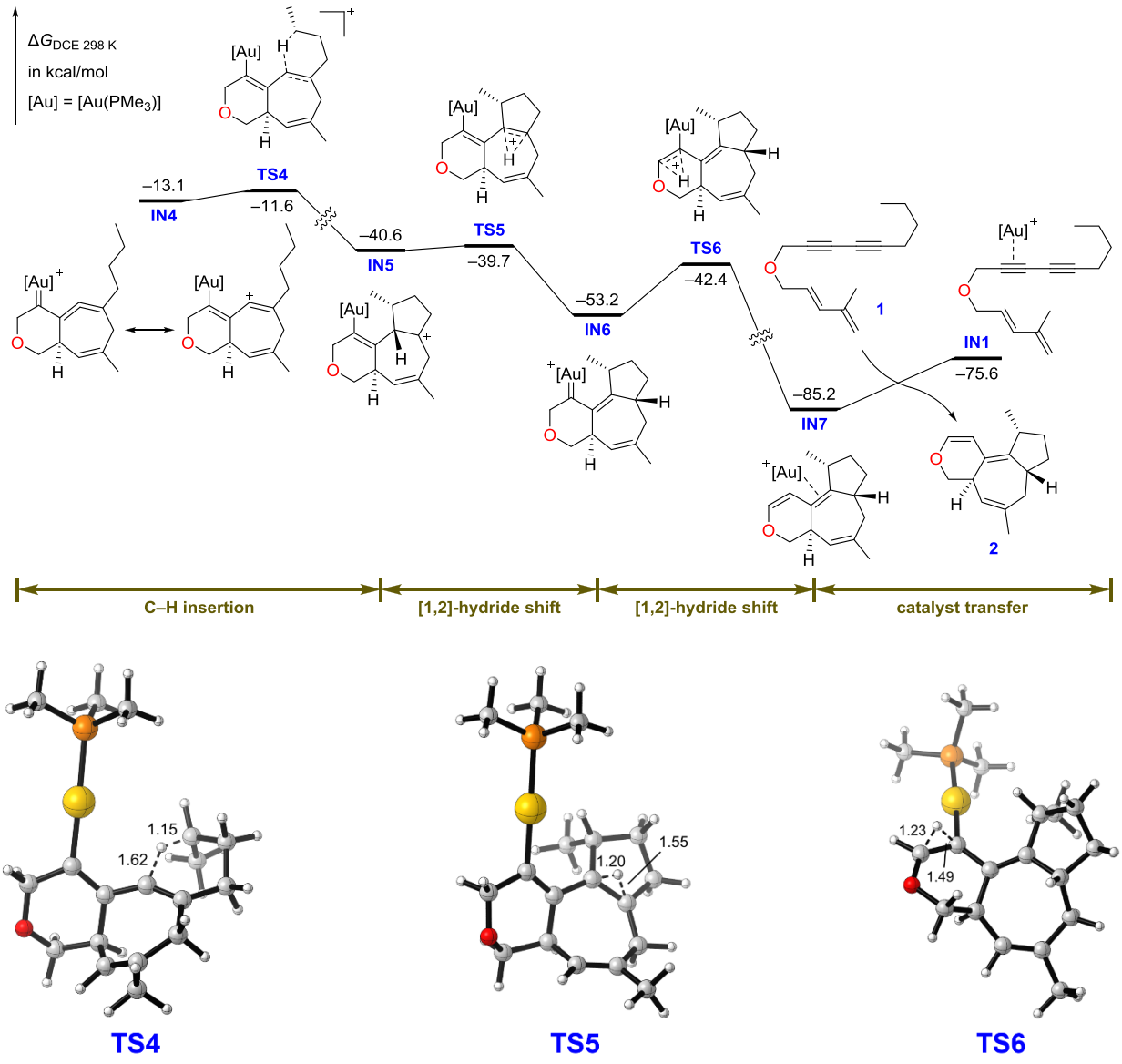

Figure 4. Gibbs energy profile for the transformation of **IN4**. Computed at the SMD(DCE)/BMK-D3(BJ)/def2-TZVPP//SMD(DCE)/PBE0/SDD-6-311G(d,p) level. Color scheme: H, white; C, gray; O, red; P, orange; Au, yellow. Bond lengths are reported in Å.

undergoes an easy [1,2]-hydride shift via **TS5**, leading to gold carbene **IN6**. It then undergoes another [1,2]-hydride shift via **TS6** with an activation Gibbs energy of 10.8 kcal/mol to form gold–product complex **IN7**,[16] which is the resting state of the catalytic cycle.[32] Finally, an endergonic catalyst transfer between **IN7** and substrate **1** furnishes gold–alkyne complex **IN1** and releases the tricyclic product **2**.[35] The overall Gibbs energy change ΔG_{rxn} is −79.4 kcal/mol (calcd from the Gibbs energy difference between **1** and **2**). The TOF-determining transition state (TDTS; TOF = turnover frequency) and the TOF-determining intermediate (TDI) are **TS1** and **IN7**, respectively. According to the energetic span model,[36] the overall activation Gibbs energy equals $\Delta\Delta G$(**TS1** − **IN7**) + ΔG_{rxn} = [15.3 − (−85.2) + (−79.4)] kcal/mol = 21.1 kcal/mol, which is in accordance with our experimental observation that the reaction took place smoothly at room temperature.

Deuterium Labeling Experiments. The proposed reaction mechanism was further supported by deuterium labeling experiments (eq 2).[14] When substrate **3** and labeled substrate **11** with deuterium atoms at the benzylic position were treated under the standard conditions, no crossover products were observed, demonstrating that the C–H insertion and the subsequent [1,2]-hydride shift are intramolecular processes.

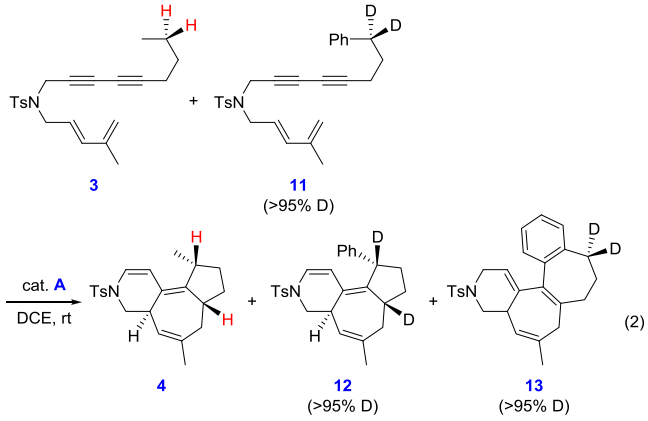

https://dx.doi.org/10.1021/jacs.9b10362
J. Am. Chem. Soc. 2020, 142, 2777–2786

Scheme 2. Possible γ-C−H Insertion Pathways for IN4[a]

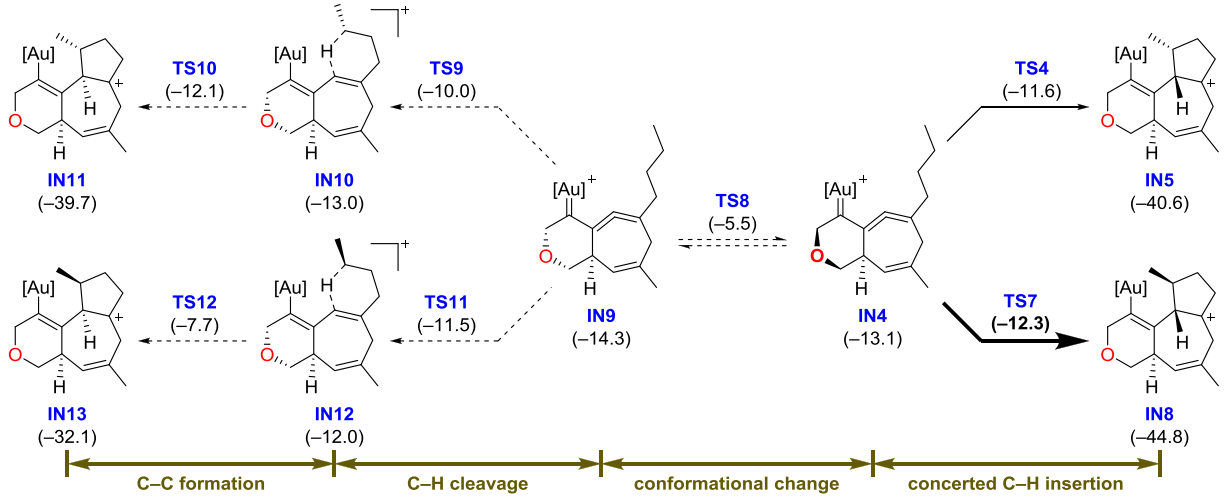

[a]Relative Gibbs energies computed at the SMD(DCE)/BMK-D3(BJ)/def2-TZVPP//SMD(DCE)/PBE0/SDD-6-311G(d,p) level are reported in kcal/mol. [Au] = [Au(PMe_3)].

Rationalization of the Selectivities in the C−H Insertion Step. *Diastereoselectivity.* There exist four possible γ-C−H insertion pathways for **IN4**, leading to the generation of four diastereomers, namely, **IN5**, **IN8**, **IN11**, and **IN13** (Scheme 2). The formation of **IN5** and **IN8** is concerted asynchronous, whereas the formation of **IN11** and **IN13** proceeds through a stepwise 1,5-hydride transfer/5-*endo*-trig cyclization pathway with the intermediacy of C−H−C three-center two-electron bonded complexes **IN10** and **IN12**, respectively. Similar phenomena have been previously observed in the theoretical investigation of the C(sp^3)−H activation by vinylidene gold complexes.[17b] DFT calculations predicted 3:1 dr and suggested that the most favored pathway is the one that furnishes **IN8** via **TS7** with a pseudoequatorial methyl group (Figure 5). But our experimentally observed diastereoselectivity suggested that the formation of **IN5** via **TS4** with a pseudoaxial methyl group should be favored. We reasoned that such a disagreement may result from the oversimplification of the ligand in our calculations. In our experiments (Scheme 1), the bulky JohnPhos was used; while in our computations, PMe_3 was used as the model ligand. To verify this hypothesis, we treated substrate **1** with Me_3PAuCl and $AgSbF_6$ and observed poor diastereoselectivity (1:1 dr).[14] This result supported our prediction that small ligand PMe_3 leads to poor stereochemical control in the present reaction.

Then, we carried out DFT calculations with the real ligand (Chart 1). We found that **TS4-JohnPhos** with a pseudoaxial methyl group is favored over **TS7-JohnPhos** with a pseudoequatorial methyl group by 1.7 kcal/mol, which is in good agreement with the experimentally observed diastereoselectivity. We attribute such a stereochemical outcome to the steric repulsion between the bulky ligand and the pseudoequatorial methyl group in **TS7-JohnPhos**, which does not exist in **TS4-JohnPhos** with a pseudoaxial methyl group. These computational results suggested that the bulky JohnPhos ligand is crucial in controlling the diastereoselectivity.

Regioselectivity. For **IN4**, besides the γ-C−H insertion pathways (Scheme 2), there are also β- and δ-C−H insertion pathways. The most favored β-, γ-, and δ-C−H insertion transition states are shown in Chart 2. All of these transition states resemble 1,*n*-hydride transfer transition states. Among them, the 1,5-hydride transfer transition state **TS7** with a six-membered-ring structure is the most favored one, which is in accordance with the previous observations that vinyl cations favor 1,5-hydride abstractions.[34]

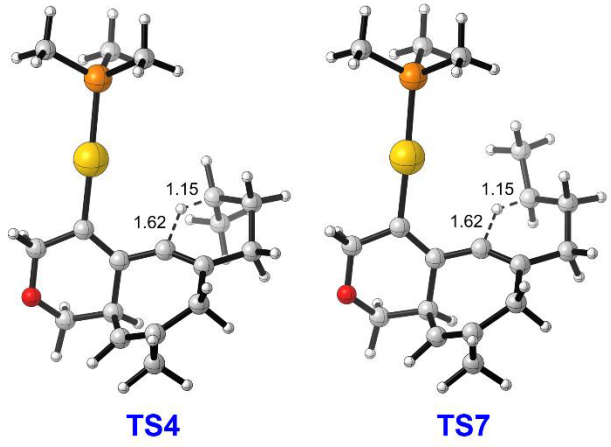

Figure 5. Optimized geometries for **TS4** and **TS7**. Computed at the SMD(DCE)/PBE0/SDD-6-311G(d,p) level. Color scheme: H, white; C, gray; O, red; P, orange; Au, yellow.

Rationalization of Regioselectivity in the Cyclopropanation Step. There is a regioselectivity issue (*endo*- versus *exo*-dig cyclizations) in the cyclopropanation step (Table 1).[2,37] Only the *endo*-dig cyclization can lead to the formation of *cis*-1-alkynyl-2-alkenylcyclopropanes (e.g., **IN2**), the precursors for the Cope rearrangement. In contrast, the *exo*-dig cyclization may lead to the generation of undesired side products and/or catalyst poisoning.

For oxygen-tethered substrate **1** and model nitrogen-tethered substrate **14** (the *N*-mesyl analog of real substrate **5**), DFT calculations suggested that the 6-*endo*-dig cyclizations are favored over the 5-*exo*-dig ones by 3.6 and 1.5 kcal/mol, respectively (Table 1, entries 1 and 2), plausibly due to the polarization of the triple bond (the distal alkynyl group is a better π-donor than the $-CH_2X-$ linker is).[37] As a result, oxygen- and nitrogen-tethered substrates underwent the desired

https://dx.doi.org/10.1021/jacs.9b10362
J. Am. Chem. Soc. 2020, 142, 2777−2786

Chart 1. Rationalization of Diastereoselectivity[a]

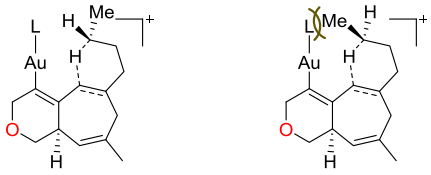

[a]Relative Gibbs energies computed at the SMD(DCE)/BMK-D3(BJ)/def2-TZVPP//SMD(DCE)/PBE0/SDD-6-311G(d,p) level are reported in kcal/mol. L = JohnPhos.

Chart 2. Most Energetically Favored β-, γ-, and δ-C−H Insertion Transition States[a]

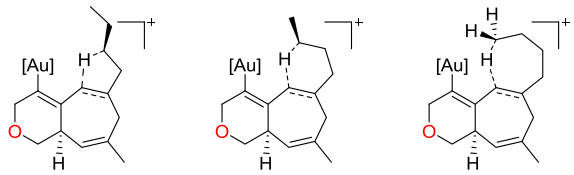

[a]Relative Gibbs energies computed at the SMD(DCE)/BMK-D3(BJ)/def2-TZVPP//SMD(DCE)/PBE0/SDD-6-311G(d,p) level are reported in kcal/mol. [Au] = [Au(PMe_3)].

6-*endo*-dig cyclization and succeeded in the catalytic tricyclization. There are many examples for gold-catalyzed 6-*endo*-dig cyclization of oxygen- and nitrogen-tethered 1,6-enynes in the literature; however, 5-*exo*-dig cyclizations are much more common for carbon-tethered 1,6-enynes.[2] Similarly, in the case of malonate-tethered substrate **7**, DFT calculations showed that the 5-*exo*-dig cyclization transition state **TS19** is favored over the 6-*endo*-dig one (**TS18**) by 3.3 kcal/mol (Table 1, entry 3). This suggested that the undesired regioselectivity (5-*exo*-dig cyclization) in the cyclopropanation step could be the reason why carbon-tethered substrate **7** failed to give the desired tricyclic product **8**.[14]

To tune the regioselectivity of carbon-tethered substrates toward the *endo*-dig cyclization, we envisioned that, by shortening the carbon tether, the *exo*-dig cyclization will lead to a highly strained fused 4,3-bicyclic intermediate and thus be inhibited. To our delight, DFT calculations supported this hypothesis. For model carbon-tethered dienediyne **15**, the 4-*exo*-dig cyclization transition state **TS21** is disfavored over the 5-*endo*-dig one (**TS20**) by 8.3 kcal/mol (Table 1, entry 4). We also tested this prediction by treating substrate **16a** under gold catalysis (Scheme 3). To our delight, the desired fused 5,7,5-tricyclic carbocycle **17a** was isolated in 91% yield. We further tested some other intramolecular nucleophiles. Both phenyl and 4-chlorophenyl substrates **16b** and **16c** underwent the anticipated cycloisomerization smoothly, affording 5,7,6,6-tetracyclic carbocycles (**17b** and **17c**) in excellent yields. Moreover, substrate **16d** with a monosubstituted diene moiety also worked very well. These results provided a new case showing that the combination of computations and experiments is a powerful tool that allows chemists to understand the reaction mechanism and to design new reactions.

Rationalization of Chemoselectivity. Finally, we tuned our attention to the understanding of the mechanistic switch between tricyclization and bicyclization (Scheme 1 and eq 1). We speculated that such a mechanistic switch may originate from the competition between Cope rearrangement and [1,2]-hydride shift (Figure 6). DFT calculations indicated that the Cope rearrangement (via **TS3**) is favored over the [1,2]-hydride shift (via **TS22**) by 2.3 kcal/mol in our case. In contrast, for Ferreira's substrate **9**, the Cope rearrangement is disfavored over the oxabicyclo[4.1.0]heptene formation by 8.6 kcal/mol (Table 2, entry 1). These computational results accord with the experimental observations (Scheme 1 and eq 1). Considering that the alkene moiety remains intact during the [1,2]-hydride shift, the substitutents on the alkene moiety only affect the activation Gibbs energy of the [1,2]-hydride shift slightly (by 1.6 kcal/mol). In contrast, they influence the activation Gibbs energy of the Cope rearrangement significantly (by 9.3 kcal/mol). We reasoned that, in Ferreira's case, the Cope rearrangement suffers from an additional loss of conjugation energy, which can be demonstrated by the significant decrease of thermodynamic driving force (−1.0 kcal/mol) as compared with that of substrate **1** (−10.4 kcal/mol).

To verify this point of view, we further investigated three model substrates (Table 2, entries 2−4). Replacement of either phenyl or methoxycarbonyl group by a hydrogen atom leads to the acceleration of the Cope rearrangement significantly (Table 2, entries 2 and 3). When both the phenyl and methoxycarbonyl groups are replaced by hydrogen atoms, the Cope rearrangement becomes favored over the [1,2]-hydride shift by 2.2 kcal/mol (Table 2, entry 4). These computational results nicely explain how the substituents affect the competition between Cope rearrangement and [1,2]-hydride shift, which is the reason behind the chemoselectivity (tricyclization versus bicyclization). Such an understanding of the substituent

Table 1. *Endo*- versus *Exo*-Dig Cyclizations[a]

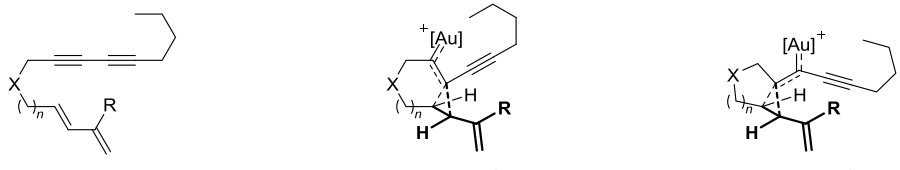

entry	X	*n*	R	substrate	*endo*-dig TS	*exo*-dig TS	$\Delta\Delta G^{\ddagger}$ (*exo*−*endo*) (kcal/mol)
1	O	1	Me	**1**	**TS1**	**TS15**	3.6
2	NMs	1	H	**14**	**TS16**	**TS17**	1.5
3	$C(CO_2Me)_2$	1	H	**7**	**TS18**	**TS19**	−3.3
4	$C(CO_2Me)_2$	0	H	**15**	**TS20**	**TS21**	8.3

[a]Computed at the SMD(DCE)/BMK-D3(BJ)/def2-TZVPP//SMD(DCE)/PBE0/SDD-6-311G(d,p) level. [Au] = [Au(PMe_3)]. TS = transition state.

https://dx.doi.org/10.1021/jacs.9b10362
J. Am. Chem. Soc. 2020, 142, 2777−2786

Scheme 3. Design of New Reactions Based upon Mechanistic Information[a]

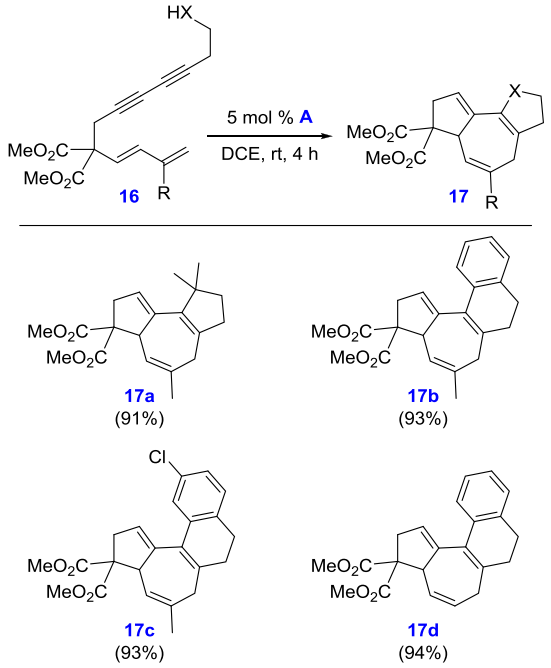

[a]Reaction conditions: dienediyne **16** (0.10 mmol), gold catalyst **A** (5 mol %), DCE (2.0 mL), rt, 4 h. Isolated yields (average of two runs) are reported in parentheses.

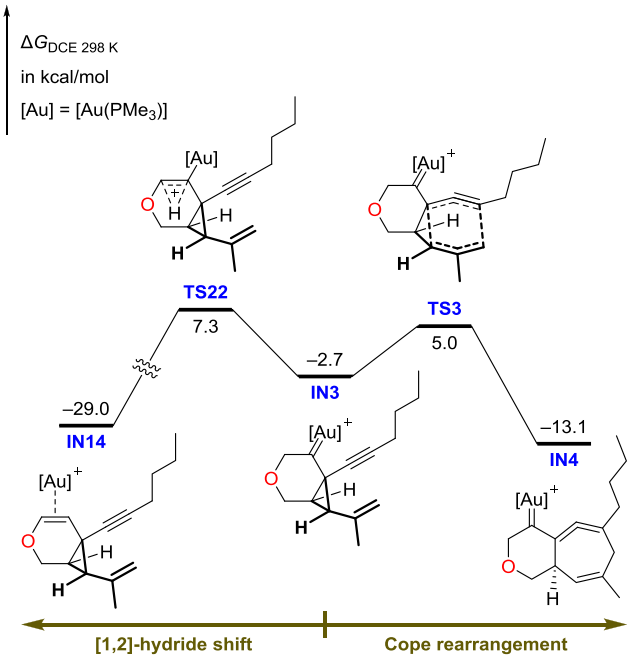

Figure 6. Competition between Cope rearrangement and [1,2]-hydride shift in our case (substrate **1**). Computed at the SMD(DCE)/BMK-D3(BJ)/def2-TZVPP//SMD(DCE)/PBE0/SDD-6-311G(d,p) level.

effect is helpful for predicting the chemical outcome of our and Ferreira's reactions as well as other catalytic cycloisomerizations involving Cope rearrangement.[4]

CONCLUSIONS

On the basis of DFT calculations and deuterium labeling experiments, we investigated the detailed reaction mechanism

Table 2. Competition between [1,2]-Hydride Shift and Cope Rearrangement[a]

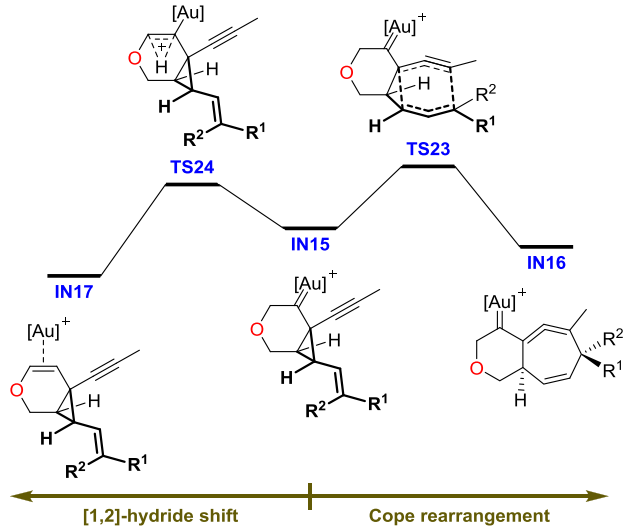

			ΔG‡; ΔG (kcal/mol)	
entry	R1	R2	[1,2]-hydride shift	Cope rearrangement
1	CO_2Me	Ph	8.4; −27.8	17.0; −1.0
2	CO_2Me	H	8.9; −28.6	11.7; −6.5
3	H	Ph	10.9; −25.4	10.6; −4.4
4	H	H	10.6; −26.1	8.4; −9.3

[a]Computed at the SMD(DCM)/BMK-D3(BJ)/def2-TZVPP//SMD-(DCM)/PBE0/SDD-6-311G(d,p) level. [Au] = [Au(PMe_3)].

for the gold-catalyzed cycloisomerization of dienediynes (Scheme 1). The elementary steps of the catalytic tricyclization involve catalyst transfer, cyclopropanation, Cope rearrangement of *cis*-1-alkynyl-2-alkenylcyclopropane, regio- and diastereoselective C−H insertion via vinyl cation, and two successive [1,2]-hydride shifts. The bulky JohnPhos ligand is found to be crucial in diastereocontrol through steric effect. These mechanistic insights on vinyl cation-induced selective C−H functionalization may help chemists design new C−H functionalization reactions. DFT calculations suggested that the reason why the fused 6,7,5-tricyclic carbocycle **8** was not formed is possibly due to the undesired regioselectivity (5-*exo*-dig) of the intramolecular cyclopropanation step. This understanding guided us to utilize dienediynes with a shortened carbon tether to inhibit the *exo*-dig cyclization so that we are able to expand the reaction scope to the construction of fused 5,7,5-tricyclic and 5,7,6,6-tetracyclic skeletons. Finally, we explored the reason why Ferreira's dienediyne **9** furnished oxabicyclo[4.1.0]heptene **10** (through cyclopropanation and [1,2]-hydride shift) other than the formal (4 + 3) cycloadduct (through tandem cyclopropanation/Cope rearrangement). DFT calculations demonstrated that the conjugated substituents (phenyl and methoxycarbonyl groups) lead to an additional loss of the conjugation energy during the Cope rearrangement process, making it disfavored over the competing [1,2]-hydride shift in Ferreira's case.

ASSOCIATED CONTENT

Supporting Information

The Supporting Information is available free of charge at https://pubs.acs.org/doi/10.1021/jacs.9b10362.

Experimental procedures, characterization data, copies of NMR spectra, and computational details (PDF)

https://dx.doi.org/10.1021/jacs.9b10362
J. Am. Chem. Soc. 2020, 142, 2777−2786

AUTHOR INFORMATION

Corresponding Author

Zhi-Xiang Yu − *Beijing National Laboratory for Molecular Sciences (BNLMS), Key Laboratory of Bioorganic Chemistry and Molecular Engineering of Ministry of Education, College of Chemistry, Peking University, Beijing 100871, China;* orcid.org/0000-0003-0939-9727; Email: yuzx@pku.edu.cn

Authors

Yi Wang − *Beijing National Laboratory for Molecular Sciences (BNLMS), Key Laboratory of Bioorganic Chemistry and Molecular Engineering of Ministry of Education, College of Chemistry, Peking University, Beijing 100871, China;* orcid.org/0000-0001-5762-5958

Pei-Jun Cai − *Beijing National Laboratory for Molecular Sciences (BNLMS), Key Laboratory of Bioorganic Chemistry and Molecular Engineering of Ministry of Education, College of Chemistry, Peking University, Beijing 100871, China*

Complete contact information is available at: https://pubs.acs.org/10.1021/jacs.9b10362

Notes

The authors declare no competing financial interest.

ACKNOWLEDGMENTS

This work was supported by the National Natural Science Foundation of China (21933003) and High-Performance Computing Platform of Peking University.

REFERENCES

(1) For selected reviews, see: (a) Hashmi, A. S. K.; Hutchings, G. J. Gold Catalysis. *Angew. Chem., Int. Ed.* **2006**, *45*, 7896−7936. (b) Li, Z.; Brouwer, C.; He, C. Gold-Catalyzed Organic Transformations. *Chem. Rev.* **2008**, *108*, 3239−3265. (c) Fürstner, A. Gold and Platinum Catalysis—A Convenient Tool for Generating Molecular Complexity. *Chem. Soc. Rev.* **2009**, *38*, 3208−3221. (d) Echavarren, A. M.; Jiménez-Núñez, E. Complexity via Gold-Catalyzed Molecular Gymnastics. *Top. Catal.* **2010**, *53*, 924−930. (e) Bhunia, S.; Liu, R.-S. Access to Molecular Complexity via Gold- and Platinum-Catalyzed Cascade Reactions. *Pure Appl. Chem.* **2012**, *84*, 1749−1757. (f) Fensterbank, L.; Malacria, M. Molecular Complexity from Polyunsaturated Substrates: The Gold Catalysis Approach. *Acc. Chem. Res.* **2014**, *47*, 953−965. (g) Dorel, R.; Echavarren, A. M. Gold(I)-Catalyzed Activation of Alkynes for the Construction of Molecular Complexity. *Chem. Rev.* **2015**, *115*, 9028−9072. (h) Pflästerer, D.; Hashmi, A. S. K. Gold Catalysis in Total Synthesis—Recent Achievements. *Chem. Soc. Rev.* **2016**, *45*, 1331−1367.

(2) For selected reviews, see: (a) Zhang, L.; Sun, J.; Kozmin, S. A. Gold and Platinum Catalysis of Enyne Cycloisomerization. *Adv. Synth. Catal.* **2006**, *348*, 2271−2296. (b) Michelet, V.; Toullec, P. Y.; Genêt, J.-P. Cycloisomerization of 1,*n*-Enynes: Challenging Metal-Catalyzed Rearrangements and Mechanistic Insights. *Angew. Chem., Int. Ed.* **2008**, *47*, 4268−4315. (c) Jiménez-Núñez, E.; Echavarren, A. M. Gold-Catalyzed Cycloisomerizations of Enynes: A Mechanistic Perspective. *Chem. Rev.* **2008**, *108*, 3326−3350. (d) Soriano, E.; Marco-Contelles, J. Mechanistic Insights on the Cycloisomerization of Polyunsaturated Precursors Catalyzed by Platinum and Gold Complexes. *Acc. Chem. Res.* **2009**, *42*, 1026−1036. (e) Obradors, C.; Echavarren, A. M. Gold-Catalyzed Rearrangements and Beyond. *Acc. Chem. Res.* **2014**, *47*, 902−912. For the first gold-catalyzed cycloisomerization of enyne-type substrates, see: (f) Hashmi, A. S. K.; Frost, T. M.; Bats, J. W. Highly Selective Gold-Catalyzed Arene Synthesis. *J. Am. Chem. Soc.* **2000**, *122*, 11553−11554.

(3) (a) Nieto-Oberhuber, C.; López, S.; Echavarren, A. M. Intramolecular [4 + 2] Cycloadditions of 1,3-Enynes or Arylalkynes with Alkenes with Highly Reactive Cationic Phosphine Au(I) Complexes. *J. Am. Chem. Soc.* **2005**, *127*, 6178−6179. (b) Nieto-Oberhuber, C.; López, S.; Muñoz, M. P.; Jiménez-Núñez, E.; Buñuel, E.; Cárdenas, D. J.; Echavarren, A. M. Gold(I)-Catalyzed Intramolecular Cyclopropanation of Dienynes. *Chem. - Eur. J.* **2006**, *12*, 1694−1702. (c) García-García, P.; Martínez, A.; Sanjuán, A. M.; Fernández-Rodríguez, M. A.; Sanz, R. Gold(I)-Catalyzed Tandem Cyclization-Selective Migration Reaction of 1,3-Dien-5-ynes: Regioselective Synthesis of Highly Substituted Benzenes. *Org. Lett.* **2011**, *13*, 4970−4973. (d) Rao, W.; Sally; Berry, S. N.; Chan, P. W. H. Gold-Catalyzed Cycloisomerization of 1,6,8-Dienyne Carbonates and Esters to *cis*-Cyclohepta-4,8-diene-Fused Pyrrolidines. *Chem. - Eur. J.* **2014**, *20*, 13174−13180. (e) Susanti, D.; Liu, L.-J.; Rao, W.; Lin, S.; Ma, D.-L.; Leung, C.-H.; Chan, P. W. H. Gold-Catalyzed Cycloisomerization and Diels-Alder Reaction of 1,4,9-Dienyne Esters to 3a,6-Methanoisoindole Esters with Pro-Inflammatory Cytokine Antagonist Activity. *Chem. - Eur. J.* **2015**, *21*, 9111−9118. (f) Zuccarello, G.; Mayans, J. G.; Escofet, I.; Scharnagel, D.; Kirillova, M. S.; Pérez-Jimeno, A. H.; Calleja, P.; Boothe, J. R.; Echavarren, A. M. Enantioselective Folding of Enynes by Gold(I) Catalysts with a Remote C_2-Chiral Element. *J. Am. Chem. Soc.* **2019**, *141*, 11858−11863.

(4) (a) Cao, Z.; Gagosz, F. Gold-Catalyzed Tandem Cycloisomerization/Cope Rearrangement: An Efficient Access to the Hydroazulenic Motif. *Angew. Chem., Int. Ed.* **2013**, *52*, 9014−9018. (b) Li, M.-R.; Wang, G.-C. Computational Study on Gold-Catalyzed (4 + 3) Intramolecular Cycloaddition of Trienyne: Mechanism, Reactivity and Selectivity. *RSC Adv.* **2016**, *6*, 73454−73468.

(5) For reviews, see: (a) Braun, I.; Asiri, A. M.; Hashmi, A. S. K. Gold Catalysis 2.0. *ACS Catal.* **2013**, *3*, 1902−1907. (b) Hashmi, A. S. K. Dual Gold Catalysis. *Acc. Chem. Res.* **2014**, *47*, 864−876. (c) Asiri, A. M.; Hashmi, A. S. K. Gold-Catalysed Reactions of Diynes. *Chem. Soc. Rev.* **2016**, *45*, 4471−4503. (d) Day, D. P.; Chan, P. W. H. Gold-Catalyzed Cycloisomerizations of 1,*n*-Diyne Carbonates and Esters. *Adv. Synth. Catal.* **2016**, *358*, 1368−1384. (e) Zhao, X.; Rudolph, M.; Hashmi, A. S. K. Dual Gold Catalysis - An Update. *Chem. Commun.* **2019**, *55*, 12127−12135.

(6) For selected reviews, see: (a) Yang, W.; Hashmi, A. S. K. Mechanistic Insights into the Gold Chemistry of Allenes. *Chem. Soc. Rev.* **2014**, *43*, 2941−2955. (b) Mascareñas, J. L.; Varela, I.; López, F. Allenes and Derivatives in Gold(I)- and Platinum(II)-Catalyzed Formal Cycloadditions. *Acc. Chem. Res.* **2019**, *52*, 465−479. For the first gold-catalyzed conversion of allenes, see: (c) Hashmi, A. S. K.; Schwarz, L.; Choi, J.-H.; Frost, T. M. A New Gold-Catalyzed C-C Bond Formation. *Angew. Chem., Int. Ed.* **2000**, *39*, 2285−2288.

(7) For a review, see: Cañeque, T.; Truscott, F. M.; Rodriguez, R.; Maestri, G.; Malacria, M. Electrophilic Activation of Allenenes and Allenynes: Analogies and Differences between Brønsted and Lewis Acid Activation. *Chem. Soc. Rev.* **2014**, *43*, 2916−2926.

(8) See ref 6 and also: (a) Trillo, B.; López, F.; Gulías, M.; Castedo, L.; Mascareñas, J. L. Platinum-Catalyzed Intramolecular [4C+3C] Cycloaddition between Dienes and Allenes. *Angew. Chem., Int. Ed.* **2008**, *47*, 951−954. (b) Trillo, B.; López, F.; Montserrat, S.; Ujaque, G.; Castedo, L.; Lledós, A.; Mascareñas, J. L. Gold-Catalyzed [4C +3C] Intramolecular Cycloaddition of Allenedienes: Synthetic Potential and Mechanistic Implications. *Chem. - Eur. J.* **2009**, *15*, 3336−3339. (c) Mauleón, P.; Zeldin, R. M.; González, A. Z.; Toste, F. D. Ligand-Controlled Access to [4 + 2] and [4 + 3] Cycloadditions in Gold-Catalyzed Reactions of Allene-Dienes. *J. Am. Chem. Soc.* **2009**, *131*, 6348−6349. (d) Alonso, I.; Trillo, B.; López, F.; Montserrat, S.; Ujaque, G.; Castedo, L.; Lledós, A.; Mascareñas, J. L. Gold-Catalyzed [4C+2C] Cycloadditions of Allenedienes, including an Enantioselective Version with New Phosphoramidite-Based Catalysts: Mechanistic Aspects of the Divergence between [4C+3C] and [4C+2C] Pathways. *J. Am. Chem. Soc.* **2009**, *131*, 13020−13030. (e) González, A. Z.; Toste, F. D. Gold(I)-Catalyzed Enantioselective [4 + 2]-Cycloaddition of Allene-Dienes. *Org. Lett.* **2010**, *12*, 200−203.

(f) Montserrat, S.; Alonso, I.; López, F.; Mascareñas, J. L.; Lledós, A.; Ujaque, G. Theoretical Study on Intramolecular Allene-Diene Cycloadditions Catalyzed by $PtCl_2$ and Au(I) Complexes. *Dalton Trans.* **2011**, *40*, 11095−11105.
(9) For selected reviews, see: (a) Hashmi, A. S. K.; Rudolph, M. Gold Catalysis in Total Synthesis. *Chem. Soc. Rev.* **2008**, *37*, 1766−1775. (b) Fürstner, A. From Understanding to Prediction: Gold- and Platinum-Based π-Acid Catalysis for Target Oriented Synthesis. *Acc. Chem. Res.* **2014**, *47*, 925−938. (c) Stathakis, C. I.; Gkizis, P. L.; Zografos, A. L. Metal-Catalyzed Cycloisomerization as a Powerful Tool in the Synthesis of Complex Sesquiterpenoids. *Nat. Prod. Rep.* **2016**, *33*, 1093−1117. (d) Hu, Y.; Bai, M.; Yang, Y.; Zhou, Q. Metal-Catalyzed Enyne Cycloisomerization in Natural Product Total Synthesis. *Org. Chem. Front.* **2017**, *4*, 2256−2275. (e) Mayans, J. G.; Armengol-Relats, H.; Calleja, P.; Echavarren, A. M. Gold(I)-Catalysis for the Synthesis of Terpenoids: From Intramolecular Cascades to Intermolecular Cycloadditions. *Isr. J. Chem.* **2018**, *58*, 639−658.
(10) Cai, P.-J.; Wang, Y.; Liu, C.-H.; Yu, Z.-X. Gold(I)-Catalyzed Polycyclization of Linear Dienediynes to Seven-Membered Ring-Containing Polycycles via Tandem Cyclopropanation/Cope Rearrangement/C-H Activation. *Org. Lett.* **2014**, *16*, 5898−5901.
(11) Nieto-Oberhuber, C.; López, S.; Muñoz, M. P.; Cárdenas, D. J.; Buñuel, E.; Nevado, C.; Echavarren, A. M. Divergent Mechanisms for the Skeletal Rearrangement and [2 + 2] Cycloaddition of Enynes Catalyzed by Gold. *Angew. Chem., Int. Ed.* **2005**, *44*, 6146−6148.
(12) For selected recent reviews on C−H functionalization, see: (a) Davies, H. M. L.; Du Bois, J.; Yu, J.-Q. C-H Functionalization in Organic Synthesis. *Chem. Soc. Rev.* **2011**, *40*, 1855−1856. (b) Yamaguchi, J.; Yamaguchi, A. D.; Itami, K. C-H Bond Functionalization: Emerging Synthetic Tools for Natural Products and Pharmaceuticals. *Angew. Chem., Int. Ed.* **2012**, *51*, 8960−9009. (c) Wencel-Delord, J.; Glorius, F. C-H Bond Activation Enables the Rapid Construction and Late-Stage Diversification of Functional Molecules. *Nat. Chem.* **2013**, *5*, 369−375. (d) Davies, H. M. L.; Morton, D. Recent Advances in C-H Functionalization. *J. Org. Chem.* **2016**, *81*, 343−350.
(13) For gold-catalyzed C−H functionalization, see ref 5 and also: (a) Hashmi, A. S. K.; Salathé, R.; Frost, T. M.; Schwarz, L.; Choi, J.-H. Homogeneous Catalysis by Gold: The Current Status of C,H Activation. *Appl. Catal., A* **2005**, *291*, 238−246. (b) Hashmi, A. S. K.; Schäfer, S.; Wölfle, M.; Diez Gil, C.; Fischer, P.; Laguna, A.; Blanco, M. C.; Gimeno, M. C. Gold-Catalyzed Benzylic C-H Activation at Room Temperature. *Angew. Chem., Int. Ed.* **2007**, *46*, 6184−6187. (c) Boorman, T. C.; Larrosa, I. Gold-Mediated C-H Bond Functionalisation. *Chem. Soc. Rev.* **2011**, *40*, 1910−1925. (d) de Haro, T.; Nevado, C. On Gold-Mediated C-H Activation Processes. *Synthesis* **2011**, *2011*, 2530−2539. (e) Nösel, P.; Nunes dos Santos Comprido, L.; Lauterbach, T.; Rudolph, M.; Rominger, F.; Hashmi, A. S. K. 1,6-Carbene Transfer: Gold-Catalyzed Oxidative Diyne Cyclizations. *J. Am. Chem. Soc.* **2013**, *135*, 15662−15666. (f) Xie, J.; Pan, C.; Abdukader, A.; Zhu, C. Gold-Catalyzed $C(sp^3)$-H Bond Functionalization. *Chem. Soc. Rev.* **2014**, *43*, 5245−5256. (g) Wang, Y.; Zarca, M.; Gong, L.-Z.; Zhang, L. A C-H Insertion Approach to Functionalized Cyclopentenones. *J. Am. Chem. Soc.* **2016**, *138*, 7516−7519. (h) Gagosz, F. Gold Vinylidenes as Useful Intermediates in Synthetic Organic Chemistry. *Synthesis* **2019**, *51*, 1087−1099.
(14) See the Supporting Information for details.
(15) (a) Dolbier, W. R., Jr.; Garza, O. T.; Al-Sader, B. H. Thermolysis of *syn*- and *anti*-Tricyclo[4.1.0.$0^{2,4}$]heptan-5-ylidene. *cis*-1-Ethynyl-2-vinylcyclopropane. *J. Am. Chem. Soc.* **1975**, *97*, 5038−5039. For a review on cyclic allenes, see: (b) Johnson, R. P. Strained Cyclic Cumulenes. *Chem. Rev.* **1989**, *89*, 1111−1124.
(16) For selected DFT studies involving [1,2]-hydride shift of gold carbenes, see ref 8 and also: (a) Shi, F.-Q.; Li, X.; Xia, Y.; Zhang, L.; Yu, Z.-X. DFT Study of the Mechanisms of In Water Au(I)-Catalyzed Tandem [3,3]-Rearrangement/Nazarov Reaction/[1,2]-Hydrogen Shift of Enynyl Acetates: A Proton-Transport Catalysis Strategy in the Water-Catalyzed [1,2]-Hydrogen Shift. *J. Am. Chem. Soc.* **2007**, *129*, 15503−15512. (b) Lemière, G.; Gandon, V.; Cariou, K.; Hours, A.; Fukuyama, T.; Dhimane, A.-L.; Fensterbank, L.; Malacria, M. Generation and Trapping of Cyclopentenylidene Gold Species: Four Pathways to Polycyclic Compounds. *J. Am. Chem. Soc.* **2009**, *131*, 2993−3006. (c) Dudnik, A. S.; Xia, Y.; Li, Y.; Gevorgyan, V. Computation-Guided Development of Au-Catalyzed Cycloisomerizations Proceeding via 1,2-Si or 1,2-H Migrations: Regiodivergent Synthesis of Silylfurans. *J. Am. Chem. Soc.* **2010**, *132*, 7645−7655. (d) Wang, T.; Shi, S.; Hansmann, M. M.; Rettenmeier, E.; Rudolph, M.; Hashmi, A. S. K. Synthesis of Highly Substituted 3-Formylfurans by a Gold(I)-Catalyzed Oxidation/1,2-Alkynyl Migration/Cyclization Cascade. *Angew. Chem., Int. Ed.* **2014**, *53*, 3715−3719. (e) Li, C.-L.; Yu, Z.-X. Asymmetric Synthesis of Azepine-Fused Cyclobutanes from Yne-Methylenecyclopropanes Involving Cyclopropanation/C-C Cleavage/Wagner-Meerwein Rearrangement and Reaction Mechanism. *J. Org. Chem.* **2019**, *84*, 9913−9928.
(17) (a) Nunes dos Santos Comprido, L.; Klein, J. E. M. N.; Knizia, G.; Kästner, J.; Hashmi, A. S. K. Gold(I) Vinylidene Complexes as Reactive Intermediates and Their Tendency to π-Backbond. *Chem. - Eur. J.* **2016**, *22*, 2892−2895. (b) Klein, J. E. M. N.; Knizia, G.; Nunes dos Santos Comprido, L.; Kästner, J.; Hashmi, A. S. K. $C(sp^3)$-H Bond Activation by Vinylidene Gold(I) Complexes: A Concerted Asynchronous or Stepwise Process? *Chem. - Eur. J.* **2017**, *23*, 16097−16103. (c) Wurm, T.; Bucher, J.; Duckworth, S. B.; Rudolph, M.; Rominger, F.; Hashmi, A. S. K. On the Gold-Catalyzed Generation of Vinyl Cations from 1,5-Diynes. *Angew. Chem., Int. Ed.* **2017**, *56*, 3364−3368.
(18) Connolly, J. D.; Hill, R. A. *Dictionary of Terpenoids*; Chapman & Hall: London, 1991.
(19) Newcomb, E. T.; Knutson, P. C.; Pedersen, B. A.; Ferreira, E. M. Total Synthesis of Gelsenicine via a Catalyzed Cycloisomerization Strategy. *J. Am. Chem. Soc.* **2016**, *138*, 108−111.
(20) Frisch, M. J.; Trucks, G. W.; Schlegel, H. B.; Scuseria, G. E.; Robb, M. A.; Cheeseman, J. R.; Scalmani, G.; Barone, V.; Mennucci, B.; Petersson, G. A.; Nakatsuji, H.; Caricato, M.; Li, X.; Hratchian, H. P.; Izmaylov, A. F.; Bloino, J.; Zheng, G.; Sonnenberg, J. L.; Hada, M.; Ehara, M.; Toyota, K.; Fukuda, R.; Hasegawa, J.; Ishida, M.; Nakajima, T.; Honda, Y.; Kitao, O.; Nakai, H.; Vreven, T.; Montgomery, J. A., Jr.; Peralta, J. E.; Ogliaro, F.; Bearpark, M.; Heyd, J. J.; Brothers, E.; Kudin, K. N.; Staroverov, V. N.; Keith, K.; Kobayashi, R.; Normand, J.; Raghavachari, K.; Rendell, A.; Burant, J. C.; Iyengar, S. S.; Tomasi, J.; Cossi, M.; Rega, N.; Millam, J. M.; Klene, M.; Knox, J. E.; Cross, J. B.; Bakken, V.; Adamo, C.; Jaramillo, J.; Gomperts, R.; Stratmann, R. E.; Yazyev, O.; Austin, A. J.; Cammi, R.; Pomelli, C.; Ochterski, J. W.; Martin, R. L.; Morokuma, K.; Zakrzewski, V. G.; Voth, G. A.; Salvador, P.; Dannenberg, J. J.; Dapprich, S.; Daniels, A. D.; Farkas, Ö.; Foresman, J. B.; Ortiz, J. V.; Cioslowski, J.; Fox, D. J. *Gaussian 09*, Revision D.01; Gaussian, Inc.: Wallingford, CT, 2013.
(21) Marenich, A. V.; Cramer, C. J.; Truhlar, D. G. Universal Solvation Model Based on Solute Electron Density and on a Continuum Model of the Solvent Defined by the Bulk Dielectric Constant and Atomic Surface Tensions. *J. Phys. Chem. B* **2009**, *113*, 6378−6396.
(22) Adamo, C.; Barone, V. Toward Reliable Density Functional Methods without Adjustable Parameters: The PBE0 Model. *J. Chem. Phys.* **1999**, *110*, 6158−6170.
(23) (a) Bühl, M.; Reimann, C.; Pantazis, D. A.; Bredow, T.; Neese, F. Geometries of Third-Row Transition-Metal Complexes from Density-Functional Theory. *J. Chem. Theory Comput.* **2008**, *4*, 1449−1459. (b) Kang, R.; Chen, H.; Shaik, S.; Yao, J. Assessment of Theoretical Methods for Complexes of Gold(I) and Gold(III) with Unsaturated Aliphatic Hydrocarbon: Which Density Functional Should We Choose? *J. Chem. Theory Comput.* **2011**, *7*, 4002−4011.
(24) (a) Andrae, D.; Häußermann, U.; Dolg, M.; Stoll, H.; Preuß, H. Energy-Adjusted *Ab Initio* Pseudopotentials for the Second and Third Row Transition Elements. *Theor. Chim. Acta* **1990**, *77*, 123−141. (b) Krishnan, R.; Binkley, J. S.; Seeger, R.; Pople, J. A. Self-Consistent Molecular Orbital Methods. XX. A Basis Set for Correlated Wave

https://dx.doi.org/10.1021/jacs.9b10362
J. Am. Chem. Soc. 2020, 142, 2777−2786

Functions. *J. Chem. Phys.* **1980**, *72*, 650−654. (c) McLean, A. D.; Chandler, G. S. Contracted Gaussian Basis Sets for Molecular Calculations. I. Second Row Atoms, Z = 11−18. *J. Chem. Phys.* **1980**, *72*, 5639−5648.
(25) (a) Zhao, Y.; Truhlar, D. G. Computational Characterization and Modeling of Buckyball Tweezers: Density Functional Study of Concave-Convex $\pi\cdots\pi$ Interactions. *Phys. Chem. Chem. Phys.* **2008**, *10*, 2813−2818. (b) Ribeiro, R. F.; Marenich, A. V.; Cramer, C. J.; Truhlar, D. G. Use of Solution-Phase Vibrational Frequencies in Continuum Models for the Free Energy of Solvation. *J. Phys. Chem. B* **2011**, *115*, 14556−14562.
(26) Boese, A. D.; Martin, J. M. L. Development of Density Functionals for Thermochemical Kinetics. *J. Chem. Phys.* **2004**, *121*, 3405−3416.
(27) (a) Grimme, S.; Ehrlich, S.; Goerigk, L. Effect of the Damping Function in Dispersion Corrected Density Functional Theory. *J. Comput. Chem.* **2011**, *32*, 1456−1465. (b) Goerigk, L.; Grimme, S. A Thorough Benchmark of Density Functional Methods for General Main Group Thermochemistry, Kinetics, and Noncovalent Interactions. *Phys. Chem. Chem. Phys.* **2011**, *13*, 6670−6688.
(28) Weigend, F.; Ahlrichs, R. Balanced Basis Sets of Split Valence, Triple Zeta Valence and Quadruple Zeta Valence Quality for H to Rn: Design and Assessment of Accuracy. *Phys. Chem. Chem. Phys.* **2005**, *7*, 3297−3305.
(29) Kang, R.; Lai, W.; Yao, J.; Shaik, S.; Chen, H. How Accurate Can a Local Coupled Cluster Approach Be in Computing the Activation Energies of Late-Transition-Metal-Catalyzed Reactions with Au, Pt, and Ir? *J. Chem. Theory Comput.* **2012**, *8*, 3119−3127.
(30) Glendening, E. D.; Reed, A. E.; Carpenter, J. E.; Weinhold, F. *NBO*, Version 3.1.
(31) Legault, C. Y. *CYLview*, 1.0b; Université de Sherbrooke, 2009; http://www.cylview.org.
(32) Besides **IN1** and **IN7**, there are many other gold complexes of substrate **1** and product **2**. But none of them is the resting state of the catalytic cycle and thus was not included in the Gibbs energy profiles. See the Supporting Information for discussion on the resting state.
(33) For reviews on vinyl cations, see: (a) Hanack, M. Vinyl Cations in Solvolysis Reactions. *Acc. Chem. Res.* **1970**, *3*, 209−216. (b) Hanack, M. Stabilized Vinyl Cations. *Acc. Chem. Res.* **1976**, *9*, 364−371. (c) Hanack, M. Mechanistic and Preparative Aspects of Vinyl Cation Chemistry. *Angew. Chem., Int. Ed. Engl.* **1978**, *17*, 333−341. (d) Stang, P. J.; Rappoport, Z.; Hanack, M.; Subramanian, L. R. *Vinyl Cations*; Academic Press, 1979. (e) Okuyama, T. Solvolysis of Vinyl Iodonium Salts. New Insights into Vinyl Cation Intermediates. *Acc. Chem. Res.* **2002**, *35*, 12−18. (f) Niggemann, M.; Gao, S. Are Vinyl Cations Finally Coming of Age? *Angew. Chem., Int. Ed.* **2018**, *57*, 16942−16944.
(34) For aliphatic C−H insertion of vinyl cations, see: (a) Schegolev, A. A.; Smit, W. A.; Roitburd, G. V.; Kucherov, V. F. Acylation of Alkynes by Cationoid Reagents with the Formation of Cyclopent-2-enone Derivatives. *Tetrahedron Lett.* **1974**, *15*, 3373−3376. (b) Biermann, U.; Koch, R.; Metzger, J. O. Intramolecular Concerted Insertion of Vinyl Cations into C-H Bonds: Hydroalkylating Cyclization of Alkynes with Alkyl Chloroformates to Give Cyclopentanes. *Angew. Chem., Int. Ed.* **2006**, *45*, 3076−3079. (c) Jin, T.; Himuro, M.; Yamamoto, Y. Brønsted Acid-Catalyzed Cascade Cycloisomerization of Enynes via Acetylene Cations and sp^3-Hybridized C-H Bond Activation. *J. Am. Chem. Soc.* **2010**, *132*, 5590−5591. (d) Zhang, F.; Das, S.; Walkinshaw, A. J.; Casitas, A.; Taylor, M.; Suero, M. G.; Gaunt, M. J. Cu-Catalyzed Cascades to Carbocycles: Union of Diaryliodonium Salts with Alkenes or Alkynes Exploiting Remote Carbocations. *J. Am. Chem. Soc.* **2014**, *136*, 8851−8854. (e) Peng, J.; Chen, C.; Chen, J.; Su, X.; Xi, C.; Chen, H. Cu-Catalyzed Arylcarbocyclization of Alkynes with Diaryliodonium Salts through C-C Bond Formation on Inert $C_{(sp3)}$-H Bond. *Org. Lett.* **2014**, *16*, 3776−3779. (f) Cleary, S. E.; Hensinger, M. J.; Brewer, M. Remote C-H Insertion of Vinyl Cations Leading to Cyclopentenones. *Chem. Sci.* **2017**, *8*, 6810−6814. (g) Popov, S.; Shao, B.; Bagdasarian, A. L.; Benton, T. R.; Zou, L.; Yang, Z.; Houk, K. N.; Nelson, H. M. Teaching an Old Carbocation New Tricks: Intermolecular C-H Insertion Reactions of Vinyl Cations. *Science* **2018**, *361*, 381−387. (h) Ikeuchi, T.; Inuki, S.; Oishi, S.; Ohno, H. Gold(I)-Catalyzed Cascade Cyclization Reactions of Allenynes for the Synthesis of Fused Cyclopropanes and Acenaphthenes. *Angew. Chem., Int. Ed.* **2019**, *58*, 7792−7796. (i) Wigman, B.; Popov, S.; Bagdasarian, A. L.; Shao, B.; Benton, T. R.; Williams, C. G.; Fisher, S. P.; Lavallo, V.; Houk, K. N.; Nelson, H. M. Vinyl Carbocations Generated Under Basic Conditions and Their Intramolecular C-H Insertion Reactions. *J. Am. Chem. Soc.* **2019**, *141*, 9140−9144. (j) Cleary, S. E.; Hensinger, M. J.; Qin, Z.-X.; Hong, X.; Brewer, M. Migratory Aptitudes in Rearrangements of Destabilized Vinyl Cations. *J. Org. Chem.* **2019**, *84*, 15154−15164.
(35) Cationic gold−π complexes may undergo facile intermolecular ligand exchange via an associative mechanism. For a review, see: Brooner, R. E. M.; Widenhoefer, R. A. Cationic, Two-Coordinate Gold π Complexes. *Angew. Chem., Int. Ed.* **2013**, *52*, 11714−11724.
(36) For a review, see: Kozuch, S.; Shaik, S. How to Conceptualize Catalytic Cycles? The Energetic Span Model. *Acc. Chem. Res.* **2011**, *44*, 101−110.
(37) (a) Alabugin, I. V.; Gilmore, K.; Manoharan, M. Rules for Anionic and Radical Ring Closure of Alkynes. *J. Am. Chem. Soc.* **2011**, *133*, 12608−12623. (b) Gilmore, K.; Alabugin, I. V. Cyclizations of Alkynes: Revisiting Baldwin's Rules for Ring Closure. *Chem. Rev.* **2011**, *111*, 6513−6556. (c) Alabugin, I. V.; Gilmore, K. Finding the Right Path: Baldwin "Rules for Ring Closure" and Stereoelectronic Control of Cyclizations. *Chem. Commun.* **2013**, *49*, 11246−11250. (d) Gilmore, K.; Mohamed, R. K.; Alabugin, I. V. The Baldwin Rules: Revised and Extended. *Wiley Interdiscip. Rev.: Comput. Mol. Sci.* **2016**, *6*, 487−514. (e) Dong, Z.; Liu, C.-H.; Wang, Y.; Lin, M.; Yu, Z.-X. Gold(I)-Catalyzed *endo*-Selective Intramolecular α-Alkenylation of β-Yne-Furans: Synthesis of Seven-Membered-Ring-Fused Furans and DFT Calculations. *Angew. Chem., Int. Ed.* **2013**, *52*, 14157−14161.

https://dx.doi.org/10.1021/jacs.9b10362
J. Am. Chem. Soc. 2020, 142, 2777−2786